NeuroImage 149 (2017) 53–62

Contents lists available at ScienceDirect

NeuroImage

journal homepage: www.elsevier.com/locate/neuroimage

GABAergic effect on resting-state functional connectivity: Dynamics under pharmacological antagonism☆

Fatima A. Nasrallah[a,b,c], Kavita Kaur D./O.Ranjit Singh[a], Ling Yun Yeow[a], Kai-Hsiang Chuang[a,c,d,*]

[a] Magnetic Resonance Imaging Group, Singapore Bioimaging Consortium, Agency for Science Technology and Research, Singapore
[b] Clinical Imaging Research Centre, National University of Singapore, Singapore
[c] Queensland Brain Institute, University of Queensland, Brisbane, QLD, Australia
[d] Centre for Advanced Imaging, University of Queensland, Brisbane, QLD, Australia

ARTICLE INFO

Keywords:
Functional MRI
Functional connectivity
Resting state network
GABAergic
Neurotransmission

ABSTRACT

Resting state functional connectivity MRI measures synchronous activity among brain regions although the mechanisms governing the temporally coherent BOLD signals remain unclear. Recent studies suggest that γ-amino butyric acid (GABA) levels are correlated with functional connectivity. To understand whether changes in GABA transmission alter functional connectivity, we modulated the GABAergic activity by a $GABA_A$ receptor antagonist, bicuculline. Resting and evoked electrophysiology and BOLD signals were measured in isoflurane-anesthetized rats under infusion of low-dose bicuculline or vehicle individually. Both somatosensory BOLD activations and evoked potentials induced by forepaw stimulation were increased significantly under bicuculline compared to vehicle, indicating increased excitability. Gradually elevated resting BOLD correlation within and between the somatosensory and visual cortices, as well as between somatosensory and caudate putamen but not within subcortical areas were found with the infusion of bicuculline. Increased cerebral blood flow was observed throughout the cortical and subcortical areas where the receptor density is high, but it didn't correlate with BOLD connectivity except in the primary somatosensory cortex. Furthermore, resting EEG coherence in the alpha and beta bands exhibited consistent change with the BOLD correlation. The increased cortico-cortical and cortico-striatal connectivity without dependence on the receptor distribution indicate that the functional connectivity may be mediated by long-range projection via the cortical and striatal GABAergic inter-neurons. Our results indicate an important role of the GABAergic system on neural and hemodynamic oscillations, which further supports the neuronal basis of functional connectivity MRI and its correlation with neurotransmission.

Introduction

Resting-state networks (RSNs) of the brain are structured spatio-temporal patterns of intrinsic oscillations. While many studies have used resting-state fMRI (rsfMRI) to measure the RSNs, the neural inference of these intrinsic oscillations and the biochemical mechanisms supporting them remain largely unknown (Leopold and Maier, 2012). In an attempt to understand the neurotransmission underpinning, we showed that functional connectivity can be modulated by alpha2-adrenergic receptor agonist and antagonist depending on the regional receptor density (Nasrallah et al., 2014a; Nasrallah et al., 2014c; Nasrallah et al., 2012b; Nasrallah et al., 2014d). Pharmacological manipulation thus provides a good way to probe the neural mechanism.

Among the neurotransmission systems, the γ-amino butyric acid (GABA) system, which is the major inhibitory system of the brain, has been a major focus as it is involved in regulating local and long-range neural synchrony as well as many neurological disorders and therapeutics (Bartos et al., 2007; Uhlhaas and Singer, 2012). When probed with midazolam, a benzodiazepine which enhances $GABA_A$ neurotransmission, an increase of BOLD signal correlation in the visual and auditory cortices but not in the motor cortex is seen (Kiviniemi et al., 2005). Ketamine, a specific NMDA receptor antagonist, reduced connectivity between nodes of the default mode network but not other areas (Scheidegger et al., 2012).

While both task activation and resting functional correlations have long been thought to reflect inhibitory and excitatory activity (Duncan

☆ Footnote: part of the results have been presented in the joint meeting of the International Society for Magnetic Resonance in Medicine – European Society for Magnetic Resonance in Medicine and Biology, Milan, Italy, 2014

* Corresponding author at: Queensland Brain Institute, University of Queensland, Brisbane, QLD, Australia.
E-mail address: kaichuang@gmail.com (K.-H. Chuang).

http://dx.doi.org/10.1016/j.neuroimage.2017.01.040
Received 11 April 2016; Accepted 17 January 2017
Available online 21 January 2017

and Congleton, 2010), the findings have been contradicting and are regional and disease dependent. For example, a positive correlation has been shown with glutamate concentrations in the perigenual anterior cingulate cortex (pACC) but not in anterior insula in healthy volunteers (Enzi et al., 2012). However, negative correlation between glutamate/glutamine level in pACC with functional connectivity was found in depression patients but not in healthy subjects (Horn et al., 2010). Besides excitatory neurotransmission, local neuronal dynamics have been shown to depend on neurochemical inhibitory tone. For example, diazepam, a nonselective GABAergic modulator, increases neural oscillations in various cortical areas (Hall et al., 2011). Negative correlation between GABA concentrations and BOLD activation in ACC under emotional or memory task, or in the motor cortex under motor learning task have been reported (Hu et al., 2013; Northoff et al., 2007; Stagg et al., 2011b). At resting state, functional connectivity has been found to correlate with glutamate and GABA levels (Duncan et al., 2013; Kapogiannis et al., 2013) as well as with the $GABA_A$ receptor binding potentials (Qin et al., 2012). Nonetheless, these static measures couldn't determine whether and how GABA transmission may alter functional connectivity.

In this study, we investigated the influence of GABAergic transmission on the dynamics of RSNs by modulating the system pharmacologically with bicuculline, an antagonist at the $GABA_A$ receptor. We aimed to determine 1) the influence of $GABA_A$ transmission on functional connectivity, 2) the role of GABAergic activity on regional or inter-regional synchrony, 3) the relationship with receptor distribution estimated by pharmacological MRI. Overall, the results show that neural and BOLD oscillations are gradually increased with the inhibition of $GABA_A$ transmission in the cortical but not the subcortical areas irrespective of receptor distribution.

Materials and methods

Experiment design

The experimental design and procedures were similar to our previous study on the adrenergic antagonist (Nasrallah et al., 2014b). Fig. 1 depicts the experimental design of the study where evoked and resting BOLD/electrophysiological activities as well as resting CBF before and after constant infusion of bicuculline (BIC)/vehicle (VEH) were measured in separate sets of animals. Somatosensory evoked potential (SEP) or fMRI was acquired first followed by resting-state measures. Resting-state activity was recorded continuously for 50 min, including a 10 min baseline followed by 40 min under BIC/VEH infusion. Afterward, the SEP or fMRI was measured again under the continuous infusion of BIC/VEH, which lasted 70 min in total. Bicuculline was administered at a very low infusion dose of 0.06 mg/kg/h. The dose was chosen by pilot experiments on the bench that didn't cause change in the arterial blood pressure and heart rate upon administration of the drug (data not shown). The vehicle group was infused with saline at the same infusion rate and volume to rule out the effects of changing blood volume and pressure. All three groups were conducted under the exact same conditions with anaesthesia maintained at 1.3% isoflurane throughout the experiment.

To measure stimulation-induced activity, two pairs of needle electrodes were inserted under the skin between digits 2 and 4 of the left and right forepaws and connected to a constant current stimulator (Isostim A320, World Precision Instruments, USA). In fMRI experiments, both forepaws were stimulated but in the SEP experiments, only one of the forepaws was stimulated to avoid forming a loop in the setup. In fMRI, the stimulus was given by a block design with 60 s resting and 20 s stimulation alternately repeated three times and adding 60 s of resting at the end. For the SEP study, stimulation was given by a block of 10 s stimulation to avoid habituation. In both studies, rectangular pulses of 9 Hz and 0.3 ms duration were used. Stimulation strengths of 2, 3, and 4 mA were used to determine the linearity of the brain responses.

Animal preparation

Fifty-two male Wistar rats (300–400 g) in total were divided into the VEH or BIC group. For the BOLD fMRI study, 16 rats were used (n=8 for each group). For the EEG, 20 rats were used (n=10 each group). For the CBF study, 16 animals were used (n=8 each group). All the experimental protocols were approved by the institutional animal care and use committee of the Biomedical Sciences Institutes, A*STAR, Singapore.

General procedure

The animals were initially anesthetized with isoflurane (3% during endotracheal intubation and surgery) via a calibrated vaporizer with a mixture of O2 and Air in a 1:2 ratio. Endotracheal intubation was performed and the rat was mechanically ventilated with a ventilator (TOPO, Kent Scientific, USA). PE-50 tubing was inserted into the tail artery for monitoring of physiological parameters and blood sampling. A 27-gauge butterfly needle was inserted into the tail vein for muscle relaxant administration. Rectal temperature was maintained at 36.5 ± 0.5 °C by a heating pad. Ventilation parameters, including respiration rate (RR), flow rate, pressure were adjusted so that arterial blood pH, pCO2, and pO2 measured (ISTAT, Abbott, USA) were maintained within physiological range. Mean arterial blood pressure (MABP) and rectal temperature were continuously monitored (Model 1025, SA Instruments Inc., USA). Artificial ventilation was necessary for maintenance of physiological parameters within the proper range. End-tidal CO2 (EtCO2) levels were continuously monitored with a capnometer (SurgiVet, Smiths Medical, USA) throughout the experiment.

MRI

After the surgical preparation, the animal was transferred to an MRI-compatible cradle (Rapid Biomedical GmbH, Germany) and its head was fixed with ear bars and a bite bar to prevent head motion. The respiration rate and pattern, and rectal temperature were monitored

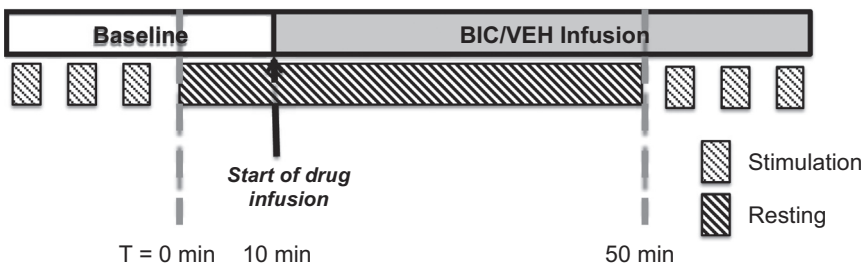

Fig. 1. Schematic representation of the time frame of the experiment. Evoked responses were studied before and under drug infusion after finishing the resting-state measurement. At time 0, continuous resting-state data acquisition was started and at 10 min, 0.06 mg/kg/h of Bicuculline (BIC) or vehicle (VEH) infusion was started. The resting-state measurement ended at 50 min, while the drug infusion still continued for measurement of evoked activity again.

using a MRI compatible physiological monitoring system (Model 1025, SA Instruments Inc., USA). The rectal temperature was maintained at ~37 °C by a feedback-controlled air heater (SA instruments Inc., USA). After full preparation, a bolus of 1.5 mg/kg pancuronium bromide (Sigma, Singapore) was given intravenously and isoflurane was decreased to 1.3%.

EEG

For intracortical EEG recordings, the rat's head was secured in a digital stereotaxic frame (Stoelting Co., USA). The skull was exposed at areas including the bregma as well as over the bilateral primary somatosensory forelimb cortex (SIFL) and the regions in front of the lambdoid suture. Two holes were drilled at the left and right SIFL (4 mm lateral and 1 mm frontal to bregma) using a drill (Foredom, Romford, UK). A third hole was drilled 10 mm posterior to the right hole for the reference electrode. Drilling was performed until the surface of the dura was revealed (approximately 1mm from the skull surface in all cases). A small opening in the dura was cut where visible blood vessels were avoided using a 27-gauge syringe needle. Then, two electrodes, fixed on a stereotaxic holder, were inserted into the cortex, ~1 mm below the brain surface, which is close to the cortical layer IV. Another electrode was inserted at 10 mm posterior to the right SIFL as the reference. Rectal temperature was monitored continuously via a thermometer and was maintained at 36.5 ± 0.5 °C using a heating pad. After full preparation, isoflurane was reduced to 1.3%.

Data acquisition

MRI

All MRI measurements were performed on a 9.4 T horizontal magnet with a bore size of 31 cm diameter (Agilent Technologies, USA). Two actively decoupled radiofrequency coils were used: a volume coil (7.2 cm inner diameter; Rapid Biomedical GmbH, Germany) for RF transmission and a custom-designed surface coil of 1.5 cm diameter as receiver. The surface coil was carefully positioned on top of the somatosensory area to ensure consistent B1 profile. A 0.5-mm diameter tube filled with water was placed on the side of the animal's head as a precautionary measure to detect any drift or other system instability. The animal's position was adjusted based on a sagittal scout image to place the primary somatosensory cortex (SI) in the magnet isocenter. The homogeneity of the magnetic field was optimized using 2nd order 3D shimming. BOLD fMRI was acquired on ten consecutive axial slices using a single-shot spin-echo echo-planar imaging (SE EPI) sequence with TR=2 s, TE=45 ms, thickness=1 mm, gap=0.1 mm, matrix size=64×64, and FOV=25.6×25.6 mm^2. For fMRI of forepaw activation, 150 scans were acquired in 5 min. Resting state was acquired for 50 min (1500 volumes).

CBF-based pharmacological MRI was measured using an optimized flow-sensitive alternating inversion recovery (FAIR) method (Nasrallah et al., 2012a). In short, the animal's brain was positioned off-center to maximize the body coverage by the volume coil for spin labelling. Shimming was optimized for the whole body. Interleaved control and label images were acquired with selective and non-selective adiabatic inversion, respectively. The images were acquired with single-shot SE EPI of TR=3.6 s, TI=1.3 s, TE=21 ms, FOV of 25.6×25.6 mm^2, matrix size of 64×64, and 7 axial slices from anterior to posterior with 2 mm thickness and no gap. Total of 834 repetitions (417 pairs) of images were acquired over 50 min.

EEG

Resting EEG and SEP were recorded under the same anesthetic and timing as the fMRI experiments. Resting EEG was recorded with a high pass filter at 0.01 Hz and SEP with a high pass filter of 0.1 Hz (MP150, Biopac, USA). The signals were amplified at a gain of 5000, sampled at 1000 Hz and recorded by the Acknowledge software (Biopac, USA).

Data processing

MRI

Functional MRI datasets were processed using custom-written scripts in Matlab (Mathworks, USA) and analysed by a software, FACT (https://sites.google.com/site/chuanglab/software/fact). All data was carefully checked for residual head movement by displaying the time series images in movie mode and calculating the center-of-mass. No movement was found in all animals. For SIFL activation, cross-correlation was computed by correlating the fMRI data with the box-car paradigm on a pixel-by-pixel basis with a correlation threshold > 0.2 and a cluster size of 4 pixels, corresponding to a corrected $p < 0.05$ determined by 3dClustSim (AFNI, National Institutes of Health, USA). Activated signal change in SIFL area was calculated and compared before vs after VEH/BIC infusion. Statistical significance was tested using ANOVA with the Bonferroni test for multiple comparisons (OriginLab Corp, USA). $P < 0.05$ was regarded as significant.

To obtain functional connectivity maps, resting-state BOLD data was pre-processed by high-pass filtering at 0.01 Hz and low-pass filtering at 0.1 Hz. It should be noted that the 0.1 Hz cutoff was only used in generating the correlation maps but not in the temporal and spectral analysis. The average signal from the ventricles, the skin and/or the external phantom were regressed out to reduce contributions from physiological noise and baseline drift. In order to improve the sensitivity while avoiding spatial blurring, spatial smoothing by a Gaussian kernel with full width at half maximum (FWHM) of 0.4 mm was applied to the data. The moment-to-moment change of connectivity was analysed by breaking the 50 min time series into ten 5-min time windows. The connectivity map was generated by seed-based correlation analysis using the time-course of a 2×2 pixel seed ROI. For the SIFL connectivity, a seed ROI was defined in the left SIFL region based on the activation map under 3 mA stimulation and by consultation with the rat brain atlas (Paxinos and Watson, 1995). Other seed ROIs were also taken in the secondary somatosensory cortex (SII), thalamus (Thal), caudate putamen (CPu), hippocampus (Hipp), and visual cortex (VC).

The connectivity strength, defined as the correlation coefficient, between functional areas was calculated between left and right SI, SII, Thal, CPu, Hipp and VC, as well as between the SI and these regions. These functional areas were defined based on the activation map and/or the brain atlas (Paxinos and Watson, 1995) in a representative slice location rather than from the seed ROIs. Since BOLD signals from large draining veins are high but less reflective of the actual neural activity, when drawing the cortical regions, caution was taken to be away from the surface of the brain so as to avoid the superficial draining veins. The time-course from each of the ROI was then extracted without applying any threshold or the low-pass filter to calculate the inter-hemispheric correlation coefficient.

The ASL data were pre-processed using a high-pass filtering method to suppress the BOLD contamination and then CBF-weighted signals were extracted (Chuang et al., 2008). The perfusion-weighted signal was then normalized to the signal of the control image in each pair. To characterize the regional effect of the drug, the area-under-curve (AUC) maps were generated from the perfusion signal integral during the drug infusion period. The mean CBF over the 5-min time window was also calculated and then normalized to the first baseline value.

EEG

The EEG data were processed using custom-written software in Matlab. SEP was calculated by averaging the first 20 epochs. The integral of the absolute amplitude of the entire evoked response was calculated. Power spectral estimation of the resting EEG signal was obtained by using the periodogram method with a sampling frequency of 1000 Hz and low-pass filtered at 49 Hz. The total power within 1 to

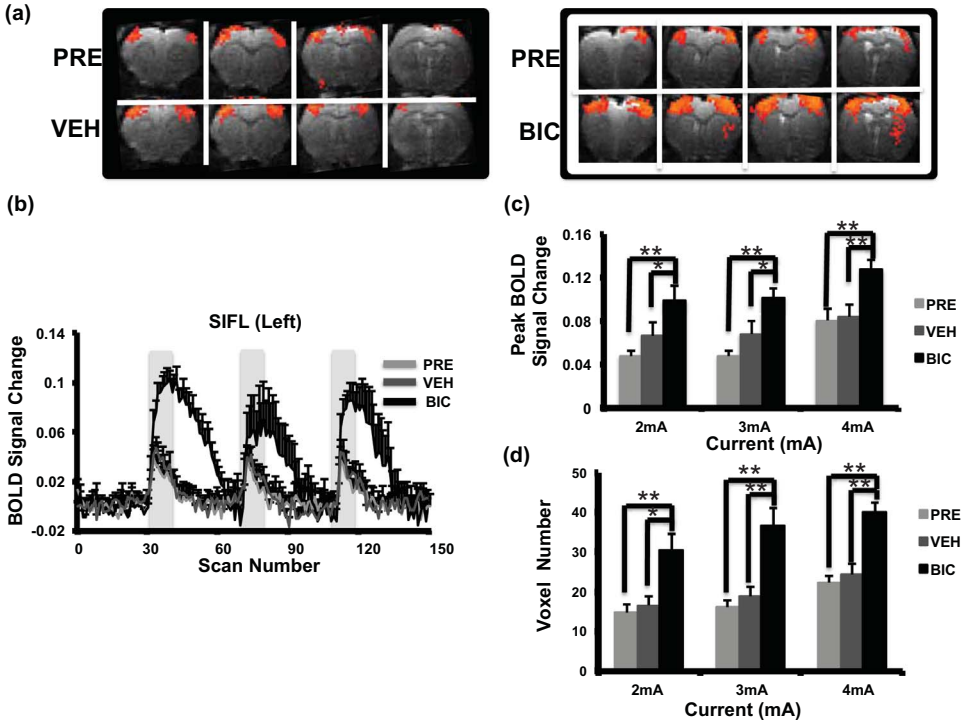

Fig. 2. Stimulation-induced BOLD activation under bicuculline. (a) Activation maps of representative animals with 9 Hz, 3 mA electrical stimulation to both forepaws before (PRE) and under vehicle (VEH) or bicuculline (BIC) infusion. Positive BOLD responses (red/yellow) were consistently observed in SI forepaw (SIFL) areas in both VEH and BIC groups. **(b)** Averaged time courses from the left SIFL areas (mean ± SEM, n=10), under the baseline (PRE; light grey), VEH (dark grey), and BIC (black). Grey bars indicate the 20 sec stimulation period. **(c)** The peak BOLD signal change under 2, 3, and 4 mA current stimulations. **(d)** The activated voxel number in the SI under 2, 3, and 4 mA current stimulations. (For interpretation of the references to color in this figure legend, the reader is referred to the web version of this article). *: $p < 0.05$; **: $p < 0.01$.

45 Hz and power within 5 predefined frequency bands based on EEG conventions (δ, 1–4 Hz; θ, 4–8 Hz; α, 8–13 Hz; β, 13–30 Hz; γL, 30–45 Hz) were calculated. Typical gamma band is in the range of 30–150 Hz. In this study, only the low gamma band (γL) was analyzed because less contribution is expected from the high gamma band since its power is much lower (Lu et al., 2007). Relative power distribution within each frequency band was obtained by normalizing with the total power. The band-limited coherence between the left and right SIFL was also calculated. Statistical significance was tested using ANOVA with the Bonferroni test for multiple comparisons. $P < 0.05$ was regarded as significant.

Results

BOLD activation under bicuculline

Similar BOLD activations were detected in the SIFL cortex at baseline and after infusing the vehicle for 40 min, indicating that the potential increase of blood volume due to continuous infusion didn't affect the BOLD signal. Under BIC, somatosensory activation was significantly increased compared to VEH and the spatial extent of the activation was increased to cover more areas such as the caudate putamen (Fig. 2a). The time-course of the BOLD activation also showed a dramatic signal increase under BIC (Fig. 2b). Compared to the BOLD change of 0.066 ± 0.012 (mean ± SEM), 0.068 ± 0.012, and 0.084 ± 0.01 under 2, 3, and 4 mA stimulation, respectively, under the VEH control, the signal change significantly increases to 0.098 ± 0.013 (p=0.0005), 0.10 ± 0.008 (p=0.0012), and 0.13 ± 0.008 (p=0.0001), respectively, under BIC (Fig. 2c). The BOLD activation area in the SI region was also increased from 16.6 ± 2.3 (pixels), 18.8 ± 2.4, and 24.3 ± 1.6 under 2, 3, and 4 mA, respectively, under VEH by almost 2 times to 30.5 ± 3.4 (p=0.009), 36.6 ± 4.3 (p=0.002), and 39.9 ± 2.7 (p=0.001) under BIC (Fig. 2d).

SEP under Bicuculline

Consistent with the BOLD activation, significant increase in SEP was observed under BIC (Fig. 3a) while the response under vehicle was similar to the baseline. The integral of the evoked response was significantly increased from 8.2 ± 1.1, 10.5 ± 0.8, and 13.5 ± 1.1 under 2, 3, and 4 mA, respectively, under VEH by about 2 times to 16.6 ± 1.8 (p=0.001), 20.1 ± 1.7 (p=0.0001), and 22.8 ± 1.4 (p=0.000004), respectively, under BIC (Fig. 3b). The integral of SEP and the peak BOLD signal change were further correlated under the baseline (PRE infusion), VEH and BIC. A good linear correlation was seen across the groups (Fig. 3c), though the relationship under VEH/BIC infusion was not as linear as the baseline.

Resting BOLD correlation under bicuculline

Similar and focal bilateral connectivity patterns were seen under VEH compared to baseline (Fig. 4a). Under BIC, a broad expansion of functional connectivity across the cerebral cortex was seen with SIFL as the seed point (Fig. 4a). The connectivity strength between the left and right SIFL was also significantly increased over time from 0.50 ± 0.03 under VEH to 0.64 ± 0.03 (p=0.007) from 5 min after the start of BIC infusion (i.e., the 15–20 min time window in Fig. 4b) and stayed elevated for 30 min (Fig. 4b).

The dynamics of connectivity between SIFL and other cortical and subcortical regions were investigated (Fig. 4c). The SI-SII connectivity was increased throughout the BIC infusion period. On the other hand, the SI-VC connectivity was only significantly increased from a sub-threshold value of 0.09 ± 0.03 at baseline to 0.33 ± 0.05 (p=0.001) after 30 min of BIC infusion. With respective to the subcortical areas, only the SI-CPu connectivity was significantly increased from 0.13 ± 0.04 under baseline to 0.24 ± 0.06 (p=0.008) after 5 min of BIC infusion and sustained towards the end. The SI-Hipp and SI-Thal connectivity remained unchanged though showing a trend of increase after 30 min.

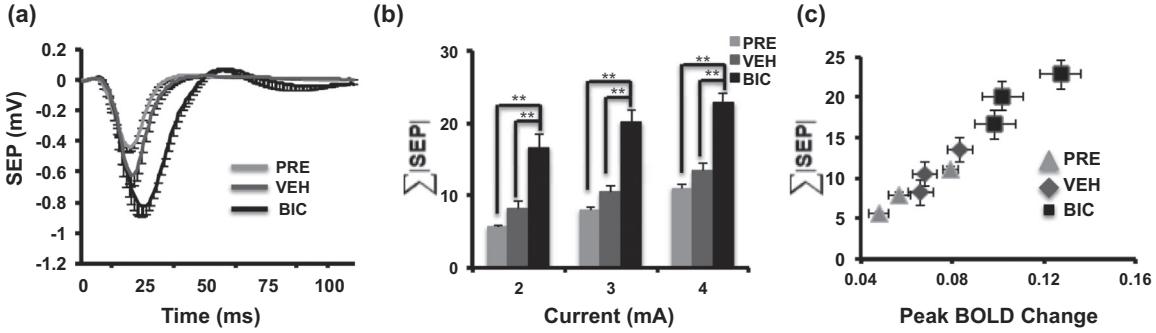

Fig. 3. Stimulation-induced Somatosensory Evoked Potential under bicuculline. (a) Averaged SEPs from the left SIFL following 3 mA stimulation (mean ± SEM, n=10) under PRE (light grey), VEH (dark grey) and BIC (black) infusion. **(b)** Integral of the SEP in PRE, VEH and BIC groups. **(c)** The relationship between the peak BOLD signal change and the SEP integral under PRE, VEH and BIC.

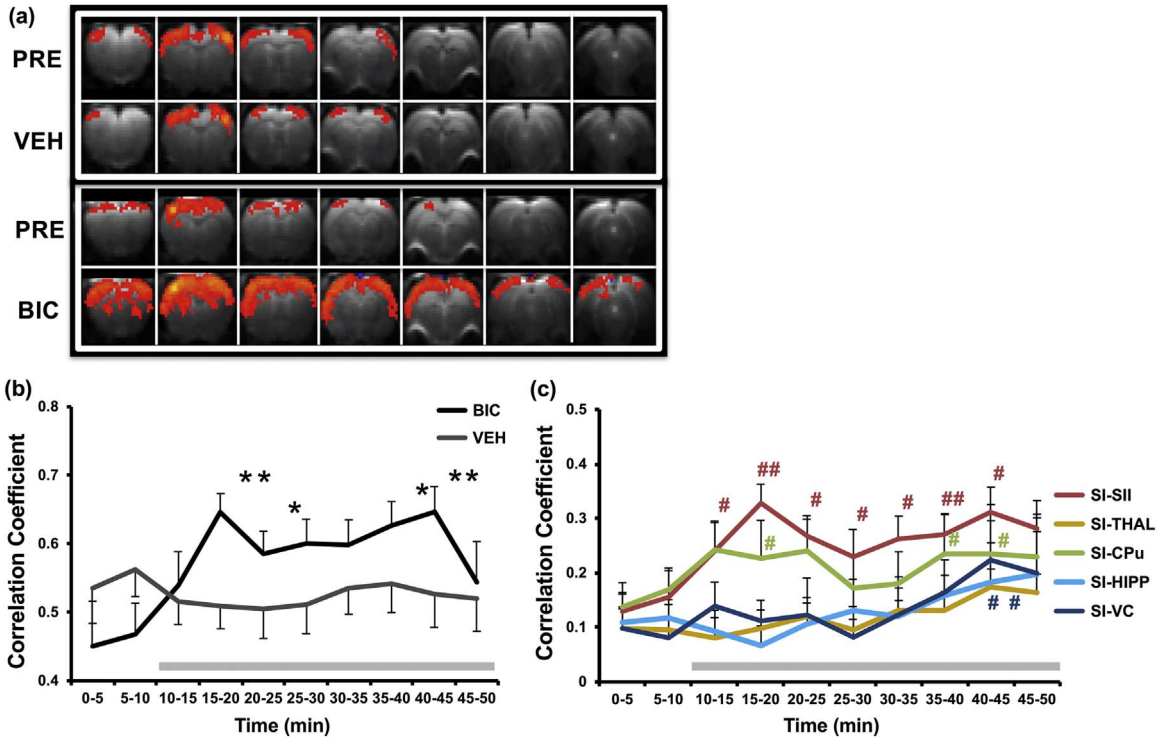

Fig. 4. Dynamics of SI connectivity under bicuculline. (a) Functional connectivity maps of the SIFL seed ROI under PRE and at different time windows during VEH or BIC infusion. **(b)** The temporal change in the correlation coefficients between the left SIFL and the right SIFL under VEH (grey) and BIC (black). Each data point in the plot represents the mean correlation coefficient over a 5 min interval. Error-bars represent SEM and asterisks represent significance difference between the BIC and VEH groups at each time window, where *: $p < 0.05$; **: $p < 0.01$. **(c)** The temporal change in the correlation coefficients between the left SIFL and other regions including SII (red), THAL (yellow), CPu (green), HIPP (light blue), and VC (blue). Each data point reflects the mean correlation coefficient over a 5 min interval. Error-bars represent SEM and asterisks represent significance difference between the PRE and the particular time window under BIC infusion, where #: $p < 0.05$; ##: $p < 0.01$. (For interpretation of the references to color in this figure legend, the reader is referred to the web version of this article).

The bilateral connectivity in other cortical and subcortical areas were shown in Fig. 5. When using cortical areas as seed points (ie, SII and VC), the connectivity expanded to other cortical areas under BIC like the case of SI. On the other hand, the connectivity from CPu, Hipp, and Thal was mostly expanded to the cortical areas. Interestingly, the dynamics of bilateral connectivity strength within a region was mostly unchanged except the VC which gradually increase and reached significance after 30 min of BIC infusion (Fig. 5b).

EEG vs BOLD correlation under bicuculline

The EEG total power in the SIFL increased significantly 5 min after the BIC infusion, peaked at 15–20 min after the start of infusion and maintained high afterward (Fig. 6a). The total power increased by about 2 folds from 0.89 ± 0.07 under VEH to 1.65 ± 0.43 under BIC (p=0.04). Comparing the BOLD correlation with EEG across the corresponding 5-min time windows, the EEG total power correlated well with BOLD (r=0.76, p=0.011) (Fig. 6b). The EEG coherence between the bilateral SIFL shows a significant decrease in the delta band (p=0.05) but an increase in the beta band (p=0.045) under BIC (Fig. 6c). Compared with BOLD correlation over the 5-min time windows, high correlation between EEG coherence and BOLD correlation was seen in the alpha (r=0.80; p=0.0052), beta (r=0.82; p=0.0036), theta (r=0.62, p=0.0063) and gamma (r=0.47, p=0.027) bands under BIC. It can be noted that although the EEG power and coherence are correlated with bilateral BOLD connectivity, there was mismatch at the first 5-min time window when BIC was started – the EEG stayed low while BOLD correlation already increased.

CBF under bicuculline

CBF-based pharmacological MRI was used to estimate the receptor

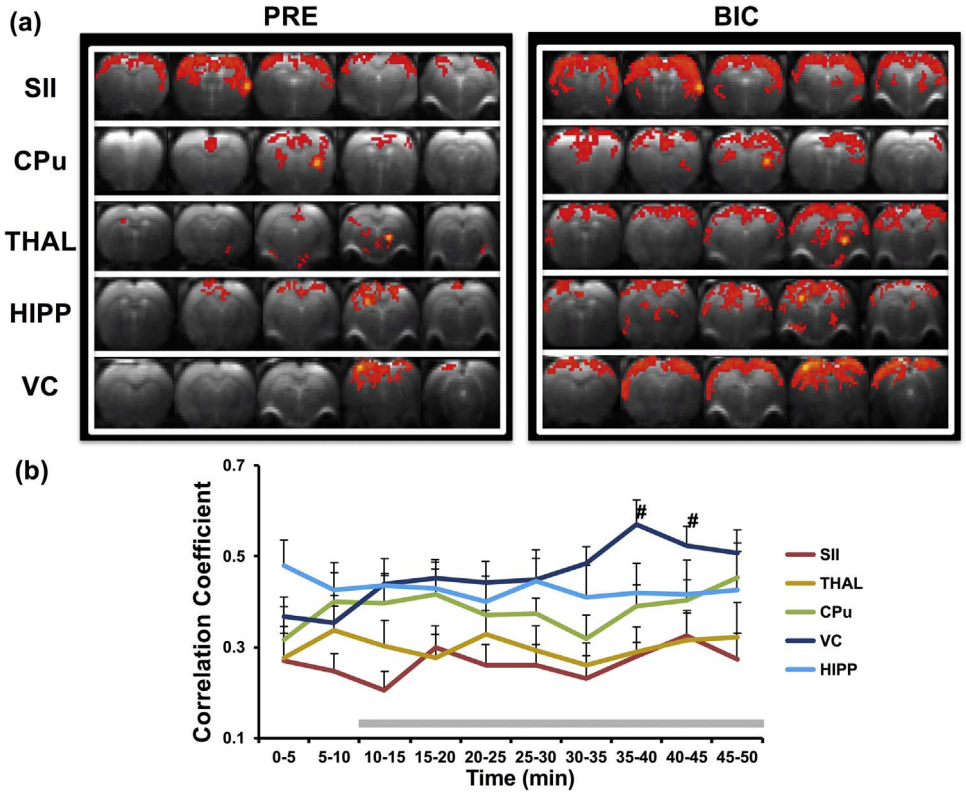

Fig. 5. Dynamics of bilateral connectivity under bicuculline. (a) Functional connectivity maps during PRE and BIC infusion with seed ROIs from the secondary somatosensory cortex (SII), caudate putamen (CPu), thalamus (THAL), hippocampus (HIPP) and visual cortex (VC) at the 35–40 min time window during BIC infusion. **(b)** The temporal change of correlation coefficients between left and right SII (red), THAL (yellow), CPu (green), HIPP (navy blue), and VC (blue). Error-bars represent SEM and asterisks represent significance difference between the PRE and particular time window during BIC infusion, where #: $p < 0.05$; ##: $p < 0.01$. (For interpretation of the references to color in this figure legend, the reader is referred to the web version of this article).

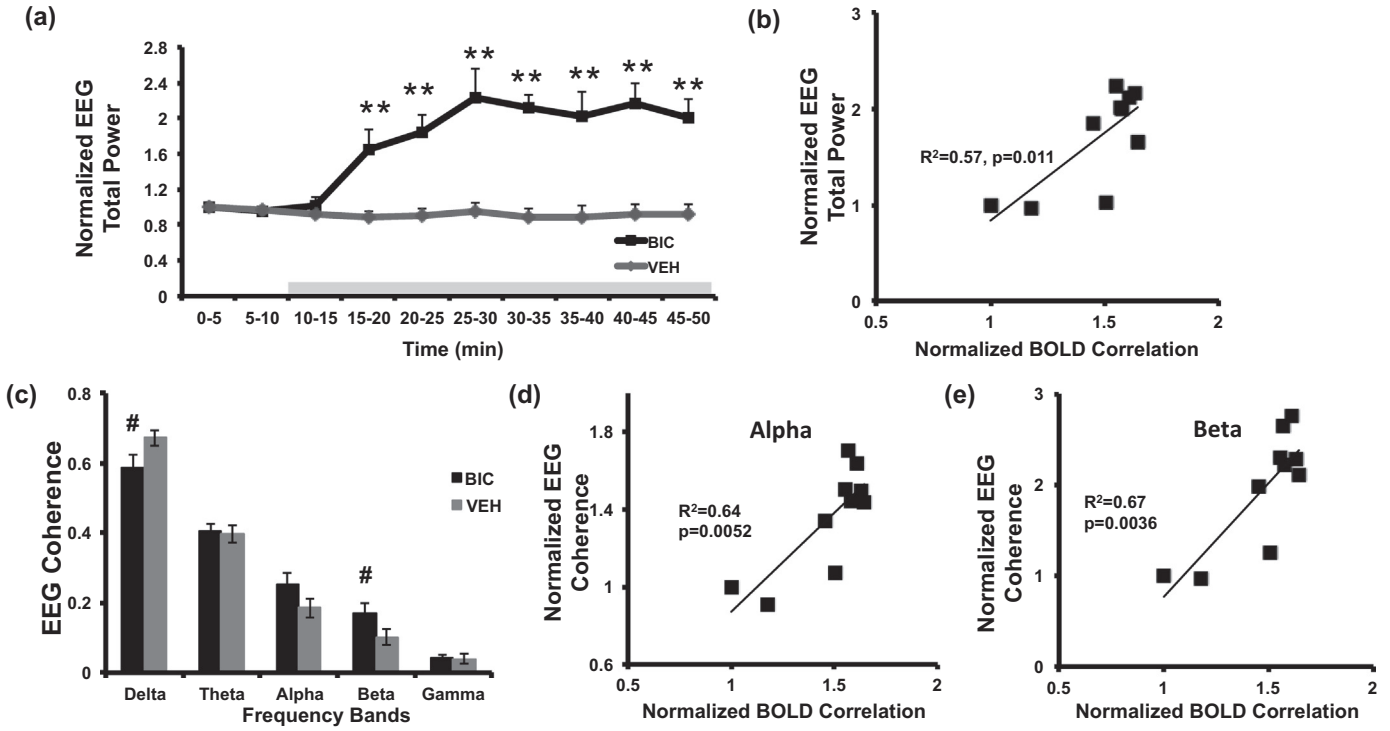

Fig. 6. Dynamics of resting EEG under bicuculline. (a) Temporal change of the normalized total EEG power measured from the SIFL area during VEH (dark gray) or BIC (black) infusion. **(b)** A linear correlation was seen between the normalized total EEG power and the normalized BOLD correlation between the left and right SIFL. **(c)** Band limited EEG coherence during VEH or BIC infusion. Significant decrease in the delta band and increase in the beta band were seen. Correlation between the normalized resting BOLD SIFL correlation and the band-limited EEG coherence in the corresponding 10 time-windows in the **(d)** alpha band and **(e)** beta band. Error-bars represent SEM and significant difference between BIC and VEH is represented by #: $p < 0.05$, ##: $p < 0.01$.

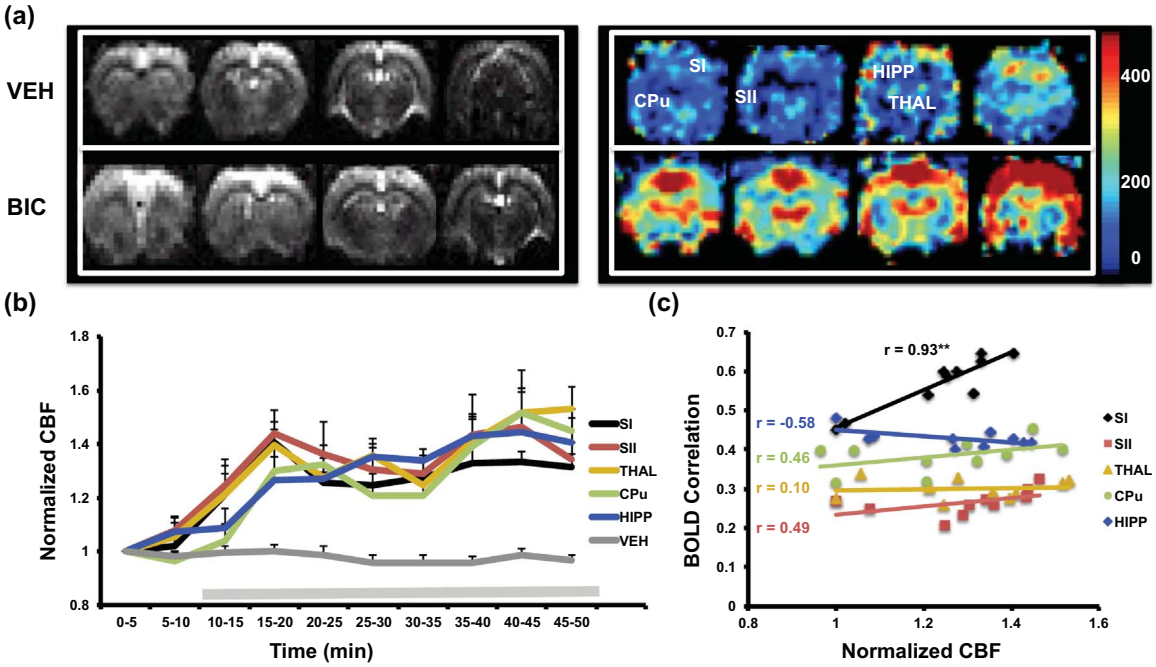

Fig. 7. Dynamics of CBF under bicuculline. (a) Representative perfusion maps under VEH (top-left) and BIC (bottom-left). The area-under-curve (AUC) maps under VEH (top-right) and BIC (bottom-right) show clear increase of CBF in CPu, HIPP, THAL, SI, and SII. **(b)** Significant increase of CBF is seen under BIC in SI (black), SII (red), THAL (yellow), CPu (green), HIPP (blue), compared to PRE. CBF under VEH doesn't change. **(c)** The bilateral BOLD correlation coefficient is correlated with CBF in SI ($p < 0.0001$) but not in SII or other regions. (For interpretation of the references to color in this figure legend, the reader is referred to the web version of this article).

distribution (Reese et al., 2000) and to assess the vascular effect of the bicuculline. Good quality of CBF was obtained over the SI, CPu to Thal (Fig. 7a). However due to the decay of perfusion signal, the CBF in the VC was poor and hence not calculated. Using the AUC map, it can be seen that BIC increased CBF highly in the Thal and CPu while slightly less in SI, SII and lowest in Hipp (Fig. 7b), reflecting the trend of $GABA_A$ receptor distribution as consistent with previous study (Reese et al., 2000). The time courses of CBF changes under bicuculline and vehicle are shown in Fig. 7c. Under vehicle, no CBF change was seen in SI. The CBF however was dramatically increased by bicuculline in all the selected areas: by 31 ± 4% in SI after 35 min of BIC infusion, by 34 ± 7% in SII, 53 ± 8% in Thal, by 45 ± 8% in CPu, and by 40 ± 9% in Hipp.

To understand the influence of CBF change on the resting BOLD correlation, the normalized CBF was correlated with bilateral BOLD correlation over the 5-min time windows (Fig. 7d). In the SI, CBF was highly correlated ($r=0.93$, $p < 0.0001$) with the BOLD connectivity measure. However, there was no correlation between CBF and bilateral BOLD connectivity in the SII, Thal, CPu and Hipp. As the CBF change would also reflect $GABA_A$ receptor density, this indicates that functional connectivity didn't correlate with the receptor distribution.

Discussion

Inhibition and excitation are the two major and inseparable activities in the brain that have major effects on the dynamics of brain circuitry and connectivity. In this work, tipping the inhibitory activity with the $GABA_A$ receptor antagonist, bicuculline, resulted in dramatic increases of BOLD signal, CBF, and EEG power, indicating increased excitatory activity and reduced inhibitions. In addition, inter-regional BOLD correlations and EEG coherence in the cortex were elevated dynamically underscoring the negative correlation between BOLD connectivity and inhibitory neurotransmission. Interestingly, the inter-regional correlations were confined to the cortex with no connectivity enhancement with subcortical regions suggesting regional-specific interactions.

Bicuculline-isoflurane interaction

A critical factor in preclinical functional MRI studies is the use of general anaesthesia to minimize distress and movement. Isoflurane is known to suppress blood pressure, respiration and neural activity (Masamoto et al., 2009). It is also demonstrated to potentiate $GABA_A$ receptor-mediated inhibition (Krasowski and Harrison, 1999, 2000; Mihic et al., 1997). Bicuculline has opposite effects on physiology at high doses (Meldrum and Nilsson, 1976) and suppresses GABAergic neurotransmission (Curtis et al., 1970). Therefore there would be potential interaction between bicuculline and isoflurane on the neural activity and functional connectivity.

A number of studies have investigated the influence of isoflurane on bicuculline induced activation. Abo et al. (2003) showed that 2% isoflurane reduced the magnitude of bicuculline-induced rCBV response in the cortex compared to 1.5% isoflurane where optimal reaction to bicuculline was observed. Detsch et al. showed that increasing the concentration of isoflurane from 0.9 to 1.9% doubled the strength of GABAergic inhibitory input to the thalamus and decreased excitatory drive of thalamocortical relay neurons by approximately 50% (Detsch et al., 2002). In this study, we used 1.3% isoflurane which is not expected to have major influence on bicuculline according to the above noted studies. While isoflurane may counteract the excitation induced by bicuculline, we found that bicuculline infusion induced a far more significant response with more than 2 folds increase in the total power of the EEG signal compared to baseline with isoflurane alone.

Since BIC and isoflurane have the opposite effects on GABA activities, one question is whether anaesthetic depth is reduced in the presence of bicuculline. In the current study, it was very hard to assess whether bicuculline did reduce the anaesthetic depth of isoflurane from the mere appearance and vital signs of the animal because all animals were paralyzed and mechanically ventilated. However, if bicuculline did reduce the anaesthetic depth of isoflurane, one would expect that the resting EEG signals under bicuculline +1.3% isoflurane would look more similar to a lower dose of isoflurane if the neural activity was suppressed to a lesser extent. By comparing intracortical recordings

under 0.7% isoflurane, BIC+1.3% isoflurane, and VEH+1.3% isoflurane, it is clear that the resting EEG signals in the BIC and VEH group are very similar with a bit of bursting that represents a deeper anaesthetic state compared to 0.7% isoflurane where the amplitude is relatively shallow representing a lighter anaesthetic state (Supplementary Figure S1). Therefore, the bicuculline dose used in this study didn't seem to affect the anaesthetic depth. It is interesting to note that bicuculline doesn't change the EEG of sleep hypnotic effects induced by flurazepam (Mendelson and Martin, 1990). Awake rodent imaging design would be needed in the future to rule out the interaction with anaesthesia.

GABAergic modulation of BOLD activation and SEP

The GABAergic system is the major inhibitory system in the brain and various attempts have been made to link changes in GABAergic transmission with underlying cellular changes. GABA levels measured by MRS were found to negatively correlate with visual activation (Muthukumaraswamy et al., 2009; Northoff et al., 2007). On the other hand, positive correlation between BOLD signal change in the visual cortex and the $GABA_A$ receptor binding potential, which represents receptor density and affinity, measured by [18 F]flumazenil PET has been reported (Qin et al., 2012). Therefore, one may predicate that decreases in GABA levels may lead to an increase in neural activation. Indeed, by reducing GABA levels with transcranial direct current stimulation (tDCS), activation in the motor area was found to increase (Stagg et al., 2011a). By directly infusing GABA into the somatosensory cortex, SEP N1 and P2 components were reduced together with a large attenuation of the hemodynamic response (Radhakrishnan et al., 2011). Consistent with the above-mentioned studies, we found that pharmacological suppression of GABA transmission with low doses of bicuculline increased the BOLD activation and SEP. Although it is difficult to estimate the effective dose at the cellular level, inhibition of GABAergic neurotransmission at very low doses has been demonstrated previously with voltage clamp recordings where tonic currents were revealed by blockade of GABA receptors with 20 μM bicuculline (Prokic et al., 2015). The extent of blocking GABAergic inhibitory signaling is also evident from the increased EEG power (Fig. 6a). Therefore, micromolar concentrations of bicuculline have significant effects on neurotransmission at the cellular level.

The main action of bicuculline is the blockade of both pre- and post-synaptic $GABA_A$ receptors. This results in decreased GABA binding at the terminals of inhibitory neurons and hence decreased inhibitory activity, which further leads to increased neural activity (Glass et al., 1980). Under the effect of bicuculline, we observe a significant increase in the SEP response and the somatosensory BOLD activation induced by electrical forepaw stimulation, consistent with previous work (Reese et al., 2000; Tsurugizawa et al., 2010). Interestingly, not only the amplitude of BOLD response but also the spatial extent of the activation was enhanced, which expanded to subcortical areas and posterior cortical regions such as the visual cortex. This may be due to the mediated disinhibitions in the brain overall (Richter et al., 2010) considering the wide distribution of $GABA_A$ receptors in the brain (Young and Chu, 1990).

GABAergic modulation on BOLD and EEG synchrony

Similar to the negative correlation observed between BOLD and SEP activation and GABA suppression, we found the suppression of inhibitory neurotransmission with bicuculline increased the resting-state functional connectivity. A previous study showed that glutamate correlated positively while GABA correlated negatively with intrinsic functional connectivity in the default mode network (Kapogiannis et al., 2013). A recent study showed that changes in GABA levels negatively correlated with a change of motor functional connectivity after a long period of motor learning (Sampaio-Baptista et al., 2015). Remarkably, the relationship was paradoxical in pre-term infants where GABA showed a positive correlation with resting connectivity measures (Kwon et al., 2014), a finding well fit with known excitatory role of GABA during development (Rheims et al., 2008). Consequently, one may postulate that blocking GABA transmission would enhance the connectivity.

On the other hand, there are studies unveil a different view. When GABAergic activity is enhanced by non-benzodiazepine (eg, zolpidem) or benzodiazepine (eg, midazolam and lorazepam) drugs, resting BOLD functional connectivity is increased in certain sensory, motor and limbic networks (Licata et al., 2013). Similar findings have been reported using MEG that elevated beta power in the motor cortex can be detected by increasing GABA activity with tiagabine, a GABA synaptic transporter blocker (Muthukumaraswamy et al., 2013). Enhanced alpha and beta band activities during both eyes open and close have also been reported with lorazepam, a benzodiazepine type of GABAergic agonist (Fingelkurts et al., 2004). These together suggest increased neural synchrony with increased inhibitory activity. Therefore, one may postulate that decreased inhibitory activity may decrease neural synchrony.

In this study, we found enhanced cortico-cortical functional connectivity, i.e, SI, SII and VC, as well as between the cortex and certain subcortical areas like CPu and Thal by blocking $GABA_A$ transmission with bicuculline. This correlated with the significantly enhanced coherence of electrophysiology from the left and right SI in the beta and alpha bands under bicuculline (Fig. 6c), indicating that the BOLD connectivity reflected neural synchrony. This functional discrepancy may be related to the particular binding site and brain regions that an allosteric GABAergic modulator (such as zolpidem) acts on compared to an orthosteric agonist or antagonist (like bicuculline). Alternatively, the increased BOLD connectivity and EEG coherence would be resulted from the overall increase in excitatory neurotransmission (Patel et al., 2004). Indeed, regional glutamate levels have been positively correlated with functional connectivity (Enzi et al., 2012; Kapogiannis et al., 2013). The enhanced cortico-striatal functional connectivity is also consistent with the known excitatory projections from the cortex (Shepherd, 2013). Direct projections from S1 to VC have been shown to be involved in multisensory interactions (Sieben et al., 2013). Since long-range GABAergic projection is sparse and limited (Tamamaki and Tomioka, 2010), such multisensory projections are likely excitatory.

GABAergic modulation of brain oscillations is regional specific

GABA has been shown to regulate neural oscillations, such as gamma oscillation (Bartos et al., 2007; Buzsáki and Wang, 2012). Several observational studies reported correlation between functional connectivity and glutamate or GABA level, or the effect of GABAergic modulators (including anesthesia that partly acts on GABAergic system) on the functional connectivity. However, the relationship differs from study to study. We observed that inhibiting the GABAergic system increased primarily cortico-cortical and cortico-striatal connectivity but not within subcortical areas or between the thalamus and cortex. This is surprising because $GABA_A$ receptors are widely distributed across the whole brain, especially in subcortical areas like the thalamus and globus pallidus, which can also be seen in the CBF-based pharmacological MRI results. Under bicuculline, thalamic connections were confined to inter and intra-thalamic nuclei, suggesting GABAergic neurons in the thalamus may not contribute to the enhanced cortical connectivity observed and the absence of cross-talk between them. However, the lack of connectivity change with thalamus may also be due to the anesthesia effect. A study compared functional connectivity between isoflurane-anethetized and awake rat showed that thalamic connectivity to other areas are suppressed at isoflurane > 1% (Liang et al., 2012; Ma et al., 2016).

Interestingly, cortico-striatal functional connectivity was enhanced by bicuculline. Such finding is consistent with previous study showing

that blockage of a specific GABAergic "tone" by intrastriatal injection of gabazine, a $GABA_A$ receptor antagonist, in the monkey striatum enhanced striatum activity and cortical oscillation (Darbin and Wichmann, 2008). Therefore, the enhanced large-scale cortical synchrony may be mediated by cortical and striatal interneurons.

GABAergic effect on CBF

Since BOLD signal is highly dependent on hemodynamic changes of CBF and cerebral blood volume (CBV), the observed changes under bicuculline may be confounded by the vascular regulation via GABA. CBF has been shown to increase by seven folds after administration of 1.2 mg/kg of bicuculline (Meldrum and Nilsson, 1976) where the $GABA_A$ receptor in particular has been suggested to be a key regulator (Chi et al., 2011; Kocharyan et al., 2007). Similarly, more than 60% increase of CBV was reported by infusing bicuculline up to 1.5 mg/kg (Mueggler et al., 2001; Reese et al., 2000). In this study, a very low dose of bicuculline (0.06 mg/kg/h) was slowly infused. This lead to less than a 50% gradual increase of CBF in all the regions investigated, especially thalamus and CPu, where the $GABA_A$ receptor densities are high. Such increase may reflect both vascular change as well as the increased neural activity and metabolic demand under bicuculline as shown in the elevated EEG power. Interestingly, while CBF showed a general increase, the CBF change did not necessarily correlate with the bilateral BOLD connectivity in the corresponding areas, such as SII, Hipp, CPu, and Thal. This mismatch connotes that the altered functional connectivity observed is very unlikely driven by underlying vascular changes. Indeed, our recent study on modulating the vascular response with CO2 and O2 shows that BOLD functional connectivity measure, especially correlation coefficient, is not affected by vascular change (Nasrallah et al., 2015).

Limitations

This current study uses a multimodal approach to understand the effect GABAergic manipulation has on resting state functional connectivity combining fMRI, CBF, and EEG measures. The cross-sectional as spite of the study therefore does pose limitations in terms of interpretation of the data. Simultaneous acquisition of EEG/fMRI would be most ideal, as it would allow correlation at each moment in each individual. However, such a dedicated setup is not readily available. Since correlation in each individual at each instance is not possible, we relied on the group average over a time window. To be able to correlate over drug dynamics, the 5-min time window was found to be suitable for calculating functional connectivity reliably. With this, a disparity in the EEG and fMRI was seen in the first 20 min of bicuculline infusion where the functional connectivity measured by fMRI reached the peak at the 2nd time window after the start of infusion, whereas EEG power reached the peak at the 4^{th} time window. Whether this is due to individual difference or the difference in the nature of the signal itself will need further investigation. While the body temperature was all maintained at physiological range, there was a minor discrepancy (~0.5°) between the MRI and the EEG experiments, likely due to faster heat dissipation on the bench compared to the enclosed MRI environment. Nonetheless, this shall not change the response to bicuculline. Finally, the anesthesia and muscle relaxant could potentially modulate multiple systems, such as nicotine receptors by pancuronium and GABA/glutamate/glycine by isoflurane, and hence presents a key drawback in terms of the interpretation of the results. Therefore awake rodent imaging would be preferable in the future to minimize these confound.

Conclusion

Many studies have shown contradicting results on the GABAergic effects on resting-state functional connectivity. Enhancing GABAergic transmission has been shown to increase functional connectivity, while higher GABA level correlates with weaker connectivity. In this study, GABAergic antagonism by bicuculline resulted in greater excitability and resting-state cortico-cortical and cortico-striatal synchrony that was confined to specific networks, independent of the global, brain-wide $GABA_A$ receptor distribution. It suggests that despite the more regionally confined characteristic of GABAergic interneuron, long-range functional connectivity change could be induced. Since altered GABAergic activity will lead to downstream changes in glutamatergic activity, further investigation shall include both systems and shall pinpoint the connectivity of the particular kind of projection between specific regions.

Acknowledgements

The work was supported by the Intramural Research program of the Singapore Bioimaging Consortium, Biomedical Sciences Institutes, Agency for Science, Technology and Research (A*STAR), Singapore.

Appendix A. Supporting information

Supplementary data associated with this article can be found in the online version at doi:10.1016/j.neuroimage.2017.01.040.

References

Abo, M., Suzuki, M., Senoo, A., Miyano, S., Yamauchi, H., Yonemoto, K., Watanabe, S., Edström, L., 2003. Influence of isoflurane concentration and hypoxia on functional magnetic resonance imaging for the detection of bicuculline-induced neuronal activation. Neuro-Signals 13, 144–149.
Bartos, M., Vida, I., Jonas, P., 2007. Synaptic mechanisms of synchronized gamma oscillations in inhibitory interneuron networks. Nat. Rev. Neurosci. 8, 45–56.
Buzsáki, G., Wang, X., 2012. Mechanisms of gamma oscillations. Neuroscience 35, 203–225.
Chi, O., Hunter, C., Liu, X., Chi, Y., Weiss, H., 2011. Effects of GABAA receptor blockade on regional cerebral blood flow and blood–brain barrier disruption in focal cerebral ischemia. J Neurol. Sci. 301, 66–70.
Chuang, K., van Gelderen, P., Merkle, H., Bodurka, J., Ikonomidou, V., Koretsky, A., Duyn, J., Talagala, S., 2008. Mapping resting-state functional connectivity using perfusion MRI. NeuroImage 40, 1595–1605.
Curtis, D., Duggan, A., Felix, D., Johnston, G., 1970. GABA, bicuculline, and central inhibition. Nature 226, 1222–1224.
Darbin, O., Wichmann, T., 2008. Effects of striatal GABA-receptor blockade on striatal and cortical activity in monkeys. J. Neurophysiol. 99, 1294.
Detsch, O., Kochs, E., Siemers, M., Bromm, B., Vahle-Hinz, C., 2002. Differential effects of isoflurane on excitatory and inhibitory synaptic inputs to thalamic neurones in vivo. Br. J. Anaesth. 89, 294–300.
Duncan, M., Congleton, M., 2010. Neural mechanisms mediating circadian phase resetting by activation of 5-HT7 receptors in the dorsal raphe: roles of GABAergic and glutamatergic neurotransmission. Brain Res. 1366, 110–119.
Duncan, N., Wiebking, C., Tiret, B., Marjańska, M., Hayes, D., Lyttleton, O., Doyon, J., Northoff, G., 2013. Glutamate concentration in the medial prefrontal cortex predicts resting-state cortical-subcortical functional connectivity in humans. PLoS One 8, e60312.
Enzi, B., Duncan, N., Kaufmann, J., Tempelmann, C., Wiebking, C., Northoff, G., 2012. Glutamate modulates resting state activity in the perigenual anterior cingulate cortex – A combined fMRI–MRS study. Neuroscience 227, 102–109.
Fingelkurts, A., Kivisaari, R., Pekkonen, E., Ilmoniemi, R., Kähkönen, S., 2004. Local and remote functional connectivity of neocortex under the inhibition influence. NeuroImage 22, 1390–1406.
Glass, J., Fromm, G., Chattha, A., 1980. Bicuculline and neuronal activity in motor cortex. Electroencephalogr. Clin. Neurophysiol. 48, 16–24.
Hall, S., Stanford, I., Yamawaki, N., McAllister, C., Rönnqvist, K., Woodhall, G., Furlong, P., 2011. The role of GABAergic modulation in motor function related neuronal network activity. NeuroImage 56, 1506–1510.
Horn, D., Yu, C., Steiner, J., Buchmann, J., Kaufmann, J., Osoba, A., Eckert, U., Zierhut, K., Schiltz, K., He, H., Biswal, B., Bogerts, B., Walter, M., 2010. Glutamatergic and resting-state functional connectivity correlates of severity in major depression - the role of pregenual anterior cingulate cortex and anterior insula. Front. Syst. Neurosci. 4.
Hu, Y., Chen, X., Gu, H., Yang, Y., 2013. Resting-state glutamate and GABA concentrations predict task-induced deactivation in the default mode network. J. Neurosci. 33, 18566–18573.
Kapogiannis, D., Reiter, D., Willette, A., Mattson, M., 2013. Posteromedial cortex glutamate and GABA predict intrinsic functional connectivity of the default mode network. NeuroImage 64, 112–119.
Kiviniemi, V., Haanpää, H., Kantola, J., Jauhiainen, J., Vainionpää, V., Alahuhta, S., Tervonen, O., 2005. Midazolam sedation increases fluctuation and synchrony of the

resting brain BOLD signal. Magn. Reson Imaging 23, 531–537.
Kocharyan, A., Fernandes, P., Tong, X., Vaucher, E., Hamel, E., 2007. Specific subtypes of cortical GABA interneurons contribute to the neurovascular coupling response to basal forebrain stimulation. J. Cereb. Blood Flow. Metab. 28, 221–231.
Krasowski, M., Harrison, N., 1999. General anaesthetic actions on ligand-gated ion channels. Cell. Mol. Life Sci. 55, 1278–1303.
Krasowski, M., Harrison, N., 2000. The actions of ether, alcohol and alkane general anaesthetics on GABA(A) and glycine receptors and the effects of TM2 and TM3 mutations. Br. J Pharmacol. 129, 731–743.
Kwon, S., Scheinost, D., Lacadie, C., Benjamin, J., Myers, E.H., Qiu, M., Schneider, K., Rothman, D., Constable, R., Ment, L., 2014. GABA, Resting-State Connectivity and the Developing Brain. Neonatology 106, 149–155.
Leopold, D., Maier, A., 2012. Ongoing physiological processes in the cerebral cortex. NeuroImage 62, 2190–2200.
Liang, Z., King, J., Zhang, N., 2012. Intrinsic organization of the anesthetized brain. J. Neurosci. 32, 10183–10191.
Licata, S., Nickerson, L., Lowen, S., Trksak, G., MacLean, R., Lukas, S., 2013. The hypnotic zolpidem increases the synchrony of BOLD signal fluctuations in widespread brain networks during a resting paradigm. NeuroImage 70, 211–222.
Lu, H., Zuo, Y., Gu, H., Waltz, J., Zhan, W., Scholl, C., Rea, W., Yang, Y., Stein, E., 2007. Synchronized delta oscillations correlate with the resting-state functional MRI signal. Proc. Natl. Acad. Sci. U S A 104, 18265–18269.
Ma, Y., Hamilton, C., Zhang, N., 2016. Dynamic Brain Connectivity Patterns in Conscious and Unconscious Brain. bioRxiv, doi: http://dx.doi.org/10.1101/075788
Masamoto, K., Fukuda, M., Vazquez, A., Kim, S., 2009. Dose-dependent effect of isoflurane on neurovascular coupling in rat cerebral cortex. Eur. J. Neurosci. 30, 242–250.
Meldrum, B., Nilsson, B., 1976. Cerebral blood flow and metabolic rate early and late in prolonged epileptic seizures induced in rats by bicuculline. Brain 99, 523–542.
Mendelson, W., Martin, J., 1990. Effects of muscimol and flurazepam on the sleep EEG in the rat. Life Sci. 47, PL99–101.
Mihic, S., Ye, Q., Wick, M., Koltchine, V., Krasowski, M., Finn, S., Mascia, M., Valenzuela, C., Hanson, K., Greenblatt, E., Harris, R., Harrison, N., 1997. Sites of alcohol and volatile anaesthetic action on GABAA and glycine receptors. Nature 389, 385–389.
Mueggler, T., Baumann, D., Rausch, M., Rudin, M., 2001. Bicuculline-induced brain activation in mice detected by functional magnetic resonance imaging. Magn. Reson. Imaging 46, 292–298.
Muthukumaraswamy, S., Edden, R., Jones, D., Swettenham, J., Singh, K., 2009. Resting GABA concentration predicts peak gamma frequency and fMRI amplitude in response to visual stimulation in humans. Proc. Natl. Acad. Sci. USA 106, 8356–8361.
Muthukumaraswamy, S., Myers, J., Wilson, S., Nutt, D., Hamandi, K., Lingford-Hughes, A., Singh, K., 2013. Elevating endogenous GABA levels with GAT-1 blockade modulates evoked but not induced responses in human visual cortex. Neuropsychopharmacology 38, 1105–1112.
Nasrallah, F., Lee, E., Chuang, K., 2012a. Optimization of flow-sensitive alternating inversion recovery (FAIR) for perfusion functional MRI of rodent brain. NMR Biomed. 25, 1209–1216.
Nasrallah, F., Lew, S., Low, A., Chuang, K., 2014a. Neural correlate of resting-state functional connectivity under α2 adrenergic receptor agonist, medetomidine. NeuroImage 84, 27–34.
Nasrallah, F., Low, S., Lew, S., Chen, K., Chuang, K., 2014b. Pharmacological insight into neurotransmission origins of resting-state functional connectivity: α2-adrenergic agonist vs antagonist. NeuroImage 103, 364–373.
Nasrallah, F., Low, S.-M.A., Lew, S., Chen, K., Chuang, K., 2014c. Pharmacological insight into neurotransmission origins of resting-state functional connectivity: α2-adrenergic agonist vs antagonist. NeuroImage 103, 364–373.
Nasrallah, F., Tan, J., Chuang, K., 2012b. Pharmacological modulation of functional connectivity: α2-adrenergic receptor agonist alters synchrony but not neural activation. NeuroImage 60, 436–446.
Nasrallah, F., Tay, H., Chuang, K., 2014d. Detection of functional connectivity in the resting mouse brain. NeuroImage 86, 417–424.
Nasrallah, F., Yeow, L., Biswal, B., Chuang, K., 2015. Dependence of BOLD signal fluctuation on arterial blood CO2 and O2: implication for resting-state functional connectivity. NeuroImage. http://dx.doi.org/10.1016/j.neuroimage.2015.05.035.
Northoff, G., Walter, M., Schulte, R., Beck, J., Dydak, U., Henning, A., Boeker, H., Grimm, S., Boesiger, P., 2007. GABA concentrations in the human anterior cingulate cortex predict negative BOLD responses in fMRI. Nat. Neurosci. 10, 1515–1517.
Patel, A., de Graaf, R., Mason, G., Kanamatsu, T., Rothman, D., Shulman, R., Behar, K., 2004. Glutamatergic neurotransmission and neuronal glucose oxidation are coupled during intense neuronal activation. J. Cereb. Blood Flow. Metab. 24, 972–985.
Paxinos, G., Watson, C., 1995. The Rat Nervous System 2nd edition. Academic Press, San Diego.
Prokic, E., Weston, C., Yamawaki, N., Hall, S., Jones, R., Stanford, I., Ladds, G., Woodhall, G., 2015. Cortical oscillatory dynamics and benzodiazepine-site modulation of tonic inhibition in fast spiking interneurons. Neuropharmacology 95, 192–205.
Qin, P., Duncan, N., Wiebking, C., Gravel, P., lyttelton, o, Hayes, D., Verhaeghe, J., Kostikov, A., Schirrmacher, R., Reader, A., Northoff, G., 2012. GABAA receptors in visual and auditory cortex and neural activity changes during basic visual stimulation. Front. Hum. Neurosci. 6.
Radhakrishnan, H., Wu, W., Boas, D., Franceschini, M.A., 2011. Study of neurovascular coupling by modulating neuronal activity with GABA. Brain Res. 1372, 1–12.
Reese, T., Bjelke, B., Porszasz, R., Baumann, D., Bochelen, D., Sauter, A., Rudin, M., 2000. Regional brain activation by bicuculline visualized by functional magnetic resonance imaging. Time-resolved assessment of bicuculline-induced changes in local cerebral blood volume using an intravascular contrast agent. NMR Biomed. 13, 43–49.
Rheims, S., Minlebaev, M., Ivanov, A., Represa, A., Khazipov, R., Holmes, G., Ben-Ari, Y., Zilberter, Y., 2008. Excitatory GABA in rodent developing neocortex in vitro. J. Neurophysiol. 100, 609–619.
Richter, D., Luhmann, H., Kilb, W., 2010. Intrinsic activation of GABAA receptors suppresses epileptiform activity in the cerebral cortex of immature mice. Epilepsia 51, 1483–1492.
Sampaio-Baptista, C., Filippini, N., Stagg, C., Near, J., Scholz, J., Johansen-Berg, H., 2015. Changes in functional connectivity and GABA levels with long-term motor learning. NeuroImage 106, 15–20.
Scheidegger, M., Walter, M., Lehmann, M., Metzger, C., Grimm, S., Boeker, H., Boesiger, P., Henning, A., Seifritz, E., 2012. Ketamine decreases resting state functional network connectivity in healthy subjects: implications for antidepressant drug action. PLoS One 7, e44799.
Shepherd, G., 2013. Corticostriatal connectivity and its role in disease. Nat. Rev. Neurosci. 14, 278–291.
Sieben, K., Röder2, B., Hanganu-Opatz, I., 2013. Oscillatory entertainment of primary somatosensory cortex encodes visual control tactile processing. J. Neurosci. 33, 5736–5749.
Stagg, C., Bachtiar, V., Johansen-Berg, H., 2011a. The role of GABA in human motor learning. Curr. Biol. 21, 480–484.
Stagg, C., Bestmann, S., Constantinescu, A., Moreno Moreno, L., Allman, C., Mekle, R., Woolrich, M., Near, J., Johansen-Berg, H., Rothwell, J., 2011b. Relationship between physiological measures of excitability and levels of glutamate and GABA in the human motor cortex. J. Physiol. 589, 5845–5855.
Tamamaki, N., Tomioka, R., 2010. Long-range GABAergic connections distributed throughout the neocortex and their possible function. Front. Neurosci. 4, 202.
Tsurugizawa, T., Uematsu, A., Uneyama, H., Torii, K., 2010. The role of the GABAergic and dopaminergic systems in the brain response to an intragastric load of alcohol in conscious rats. Neuroscience 171, 451–460.
Uhlhaas, P., Singer, W., 2012. Neuronal dynamics and neuropsychiatric disorders: toward a translational paradigm for dysfunctional large-scale networks. Neuron 75, 963–980.
Young, A., Chu, D., 1990. Distribution of GABAA and GABAB receptors in mammalian brain: potential targets for drug development. Drug Dev. Res. 21, 161–167.